14 Aug 2008, 2:15pm - 4:00pm

# A Combination of Artificial Ground Freezing and Grouting for the Excavation of a Large Size Tunnel Below Groundwater

Vittorio Manassero
*Trevi Group, Cesena, Italy*

Giuseppe Di Salvo
*Trevi Group, Cesena, Italy*

Fabio Giannelli
*Astaldi, Roma, Italy*

Giuseppe Colombo
*Metropolitana Milanese, Milano, Italy*

# A COMBINATION OF ARTIFICIAL GROUND FREEZING AND GROUTING FOR THE EXCAVATION OF A LARGE SIZE TUNNEL BELOW GROUNDWATER

**Vittorio Manassero**
Trevi Group
Cesena - Italy

**Giuseppe Di Salvo**
Trevi Group
Cesena – Italy

**Fabio Giannelli**
Astaldi
Roma – Italy

**Giuseppe Colombo**
Metropolitana Milanese
Milano – Italy

ABSTRACT

Within the Metro Line 1 extension project in Napoli (Italy), the *service tunnel* at Toledo station was one of the most critical sections of the project. The 13m wide, 17m high, 40m long tunnel is located downtown under a deeply urbanized area. It was excavated starting from an access shaft and from this tunnel four platform tunnels are under excavation. The geology of the site is characterized by volcanic soils: loose *pozzolana* silty sand and tuff. The underground works were carried out under a hydrostatic head of 27 m. In order to allow a safe and substantially dry excavation, soil/rock improvements were carried out by a combination of two different methods: cement and chemical grouting at the sides and invert (in *tuff*) and Artificial Ground Freezing (AGF) at the crown (in *pozzolana*). The treatments were carried out both from a drift located approximately 10 m above the crown and from the access shaft. The grouting process was controlled and monitored by a computerized system. To check the development and the efficacy of the freezing process, suitable sensors and automatic data acquisition and recording systems were installed. The variation of the temperature within the soil and the cooling fluids were monitored during the entire freezing operation.

INTRODUCTION

The Metro Line 1 extension in Napoli (Italy) links the terminal of *Dante Square* with *Garibaldi Square* (where the Central Railway Station is located) and the Business Center. The new stretch of the Metro Line, called *tratta bassa* (low stretch), runs along the coastline, where the commercial harbour is situated. It includes five new stations and two twin rail tunnels with a total length of 5 Km. The general layout of the whole Line 1 is shown in Fig. 1. The final layout of the Line 1, once completed, will form a closed ring around and through the town. It will be a modern and efficient underground system. The five stations are all located downtown, in a deeply urbanized area. The geology of the site is characterized by volcanic soils: loose volcanic silty sand (*pozzolana*) underlain by volcanic soft rock (*tuff*). From an excavation point of view, the *pozzolana* sand is very dangerous, especially in presence of water, due to the absence of any cohesion. The *tuff* is a prevalently soft, elastic, homogeneous and compact rock.
In order to minimize the effects induced by the excavation on the existing buildings, the rail tunnels where designed entirely within the massive tuff rock, avoiding the excavation through the loose soil where possible. This meant to run the line up to 40 m below the ground level with a hydrostatic head up to 40 m.
A longitudinal section along the entire line axis showing the position of the rail tunnels in relation to the position of the top of the massive rock layer is illustrated in Fig 2.

The stations are in general composed of one access shaft, four platform tunnels and four pedestrian access tunnels.
Four stations out of five have the access shaft centered on the twin rail tunnels, with all the station tunnels excavated starting from this central shaft. The platform tunnels are generally 11 m wide, 9.5 m high and 50 m long, whereas the pedestrian tunnels are generally 6 m x 6.5 m x 40 m.


*Fig. 1. Metro Line 1 of Napoli: General Layout*

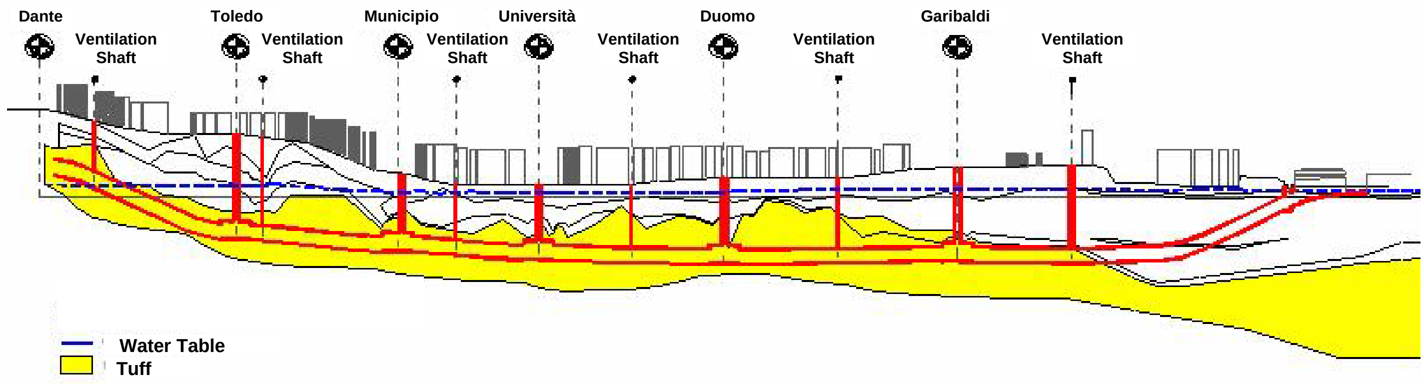


*Fig. 2. Longitudinal section along the line tunnel axis.*

Only the Toledo Station has the shaft off-centered and requires a different construction sequence: first, a large size *service tunnel* is excavated, starting from the access shaft, and then all the station tunnels are constructed starting from it. A picture that shows the close position of the shaft to the adjacent buildings is shown in Fig. 3**.** A 3-D schematic that shows the shaft and the tunnels system is presented in Fig 4 (pedestrian access tunnels are not shown in this figure).

For all the platform and pedestrian tunnels, the Artificial Ground Freezing (AGF) technique is applied as temporary soil/rock improvement. The AGF treatment contributes to the formation of a closed chamber. The boundaries of the chamber are the horizontal pseudo-cylindrical frozen ground shell, the shaft vertical wall and an end plug of improved soil.

Only for the Toledo *service tunnel* the pseudo-cylindrical shell is achieved by a combination of two different soil improvement methods: grouting at the sides and invert (in *tuff*) and AGF at the crown (in *pozzolana*). Cement and chemical grouting is carried out through sub-vertical grouting pipes, installed from a drift located some 10 m above the crown and just above the water table. The AGF is carried out through freeze-lances installed both horizontally from the access shaft and sub-vertically from the drift. The closed chamber is completed by an end plug made by jet grouting and grouting.

## GEOLOGICAL AND GEOTECHNICAL ASPECTS

Under the first 10 m, characterized by a significant presence of anthropic fill, the soil sequence shows the presence of a volcanic deposit, whose formation can be dated starting 12,000 years ago [Cavagna et al., 2004]. This deposit has a chaotic structure due to the pyroclastic flow during the formation phase. It consists of a loose soil in the upper part (*pozzolana*) and soft rock in the lower part (*Napolitan yellow tuff*). The presence of random cracks in the tuff is likely. These cracks, formed during the cooling process of the pyroclastic matrix, could be very dangerous for the excavation works, since the estimated permeability is much higher than the sound tuff. During the site investigation program several undisturbed samples of tuff were recovered and tested. The laboratory analysis included the measure of shear resistance, Young

*Fig. 3. Picture of the Toledo Station Site.*

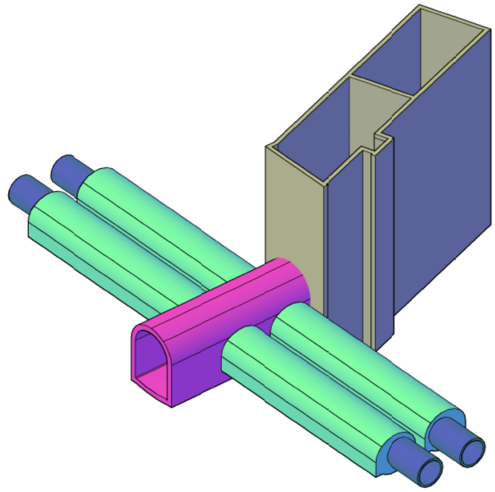

*Fig. 4. 3-D view of the Toledo Station and tunnel system.*

Modulus, porosity and specific weight. Several *in situ* tests were also carried out. The permeability was measured using the Lugeon method.

The *yellow tuff* shows a linear elastic behaviour at the stress level present at the depth of the tunnels under construction. The elastic modulus E is between 1500 and 2000 MPa. The main properties of the *yellow tuff* are shown in the Table 1**.** Above this massive rock formation there is a thick layer of silty sand (*pozzolana)*, characterized by a particularly small grain size. The pozzolana was investigated by both *in situ* tests and laboratory analysis on samples recovered at different depths. The properties of the *pozzolana* are shown in Table 2.

In order to improve the knowledge of the actual hydraulic conductivity of the tuff, a further series of Lugeon tests was carried out during construction. The results of these tests show that the permeability of the sound tuff samples, well known from several laboratory tests, is very different from the in-situ permeability of the tuff mass.

An horizontal borehole 45 m long, carried out within the core of the *service tunnel* from the Toledo shaft, revealed the presence of a crack system, with different orientation and different spacing (from tenths of millimetre up to centimetres), that together with particularly weathered zones gives the mass an average global permeability coefficient comparable with the one of a loose soil. Table 3 presents the results of these Lugeon tests. Figure 5 shows a picture of a typical box containing the recovered tuff samples.

*Table 1: Property of Yellow Tuff.*

| **Characteristic** | **Average value** |
|---|---|
| Dry specific weight $\gamma_d$ [KN/m$^3$] | 11 - 12 |
| Saturated specific weight $\gamma_{sat}$ [KN/m$^3$] | 16 - 17 |
| Effective specific weight $\gamma'$ [KN/m$^3$] | 6 - 7 |
| Porosity | 0,55 |
| Permeability k [cm/s] | $10^{-4}$ - $10^{-5}$ |
| Unconfined compressive strength $\sigma_{UCS}$ [MPa] | 3,0 |
| Drained cohesion c' [MPa] | 0,8 - 1,0 |
| Angle of shear strength φ' [°] | 27° - 28° |
| Young Modulus E [MPa] | 1500 |
| Poisson coefficient v' [KN/m$^3$] | 0,3 |
| $K_0$ | 0,5 |

*Table 2: Properties of Pozzolana*

| **Characteristic** | **Average value** |
|---|---|
| Dry specific weight $\gamma_d$ [KN/m$^3$] | 14,5 |
| Saturated specific weight $\gamma_{sat}$ [KN/m$^3$] | 19,0 |
| Water immersed specific weight $\gamma'$ [KN/m$^3$] | 9,0 |
| Porosity | 0,4 |
| Drained cohesion c' [MPa] | 0 |
| Angle of shear strength φ' [°] | 38° |
| Poisson coefficient v' [KN/m$^3$] | 0,3 |
| $K_0$ | 0,5 |

SERVICE TUNNEL DESIGN

The Toledo *service tunnel* is 13m wide, 17m high and 40m long. This tunnel has both a temporary and a permanent function. The temporary function is to provide suitable room to build the platform and the pedestrian tunnels. The permanent function will be to allow the transit of people from one track to the other, once the station is completed and the bottom part of the *service tunnel* becomes part of the platform. Furthermore, at the end of the *service tunnel* a 200 m pedestrian tunnel will be constructed to link the station with a higher quarter of Napoli (*Quartieri Spagnoli).*

The *service tunnel* is a large tunnel under an urbanized area. The main construction difficulties to be taken into consideration are (Figure 6):

- the proximity of the tunnel crown to the building foundations and various utilities, in particular to one main sewer;

*Table 3: Lugeon test results*

| **Depth** | **Rec.** | **RQD** | **Q** | **Lugeon Unit** | | **Permeability k (m/s)** | |
|---|---|---|---|---|---|---|---|
| | **%** | **%** | **(l/s)** | **Lam.** | **Turb.** | **Lam.** | **Turb** |
| 0-10 | 92,2 | 68,0 | | | | | |
| 5-10 | 87,8 | 35,4 | 4,37 | 35 | 22 | 5,8E-06 | 3,7E-06 |
| 10-15 | 94,6 | 68,8 | 5,50 | 41 | 25 | 6,8E-06 | 4,2E-06 |
| 15-20 | 89,8 | 14,8 | 5,99 | 52 | 29 | 8,6E-06 | 4,8E-06 |
| 20-25 | 83,8 | 28,8 | 6,50 | 38 | 24 | 6,3E-06 | 4,0E-06 |
| 25-30 | 98,2 | 82,2 | 6,50 | 33 | 22 | 5,5E-06 | 3,7E-06 |
| 30-35 | 85,5 | 55,6 | 7,36 | 25 | 18 | 4,2E-06 | 3,0E-06 |
| 35-40 | 90,2 | 63,4 | 7,69 | 36 | 23 | 6,0E-06 | 3,8E-06 |
| 40-45 | 91,2 | 59,8 | 9,44 | 45 | 27 | 7,5E-06 | 4,5E-06 |


*Fig.5. Typical tuff samples recovered by coring*

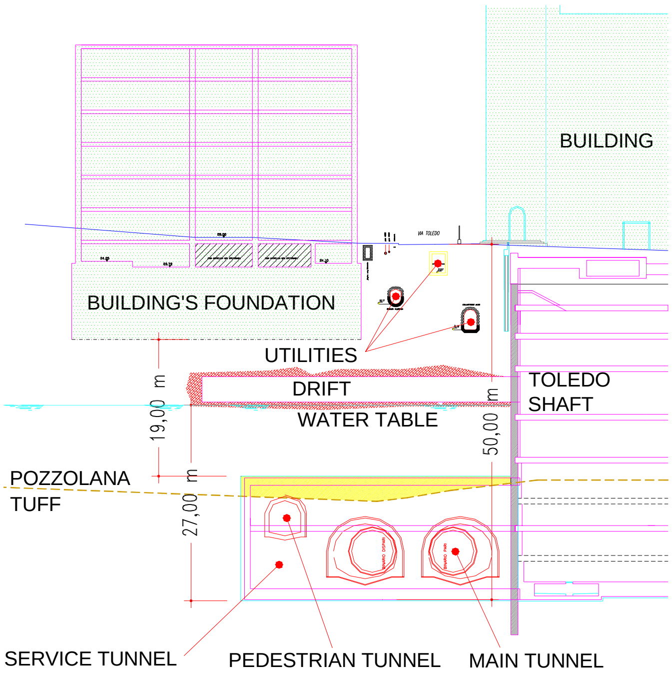


*Fig. 6. Longitudinal section of the Service Tunnel and its position with respect to buildings, utilities and water-table.*

- the water table is located 27 m above the tunnel invert;
- the significant presence at the top of the tunnel of loose soil (*pozzolana* sand);
- the large size of the tunnel.

The mutual position between the shaft and the *service tunnel* prevented the drilling of all the boreholes from the shaft through the sides and the invert of the tunnel to be excavated. The design of the soil improvement adopted for all the other tunnels (AGF all around the whole tunnel section) was not applicable to the *service tunnel*. It became necessary to look for different techniques for the soil/rock improvement. The average global hydraulic conductivity of the tuff, assessed by the additional Lugeon tests, showed that the tuff was suitable for conventional grouting. This allowed to conceive

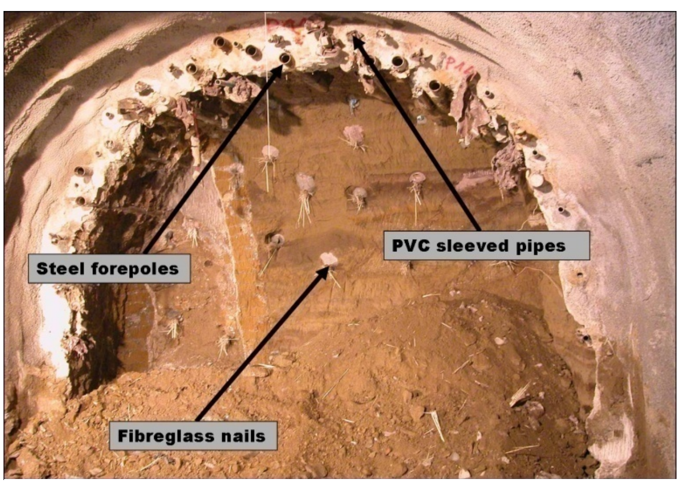


*Fig.7. Drift during its excavation*

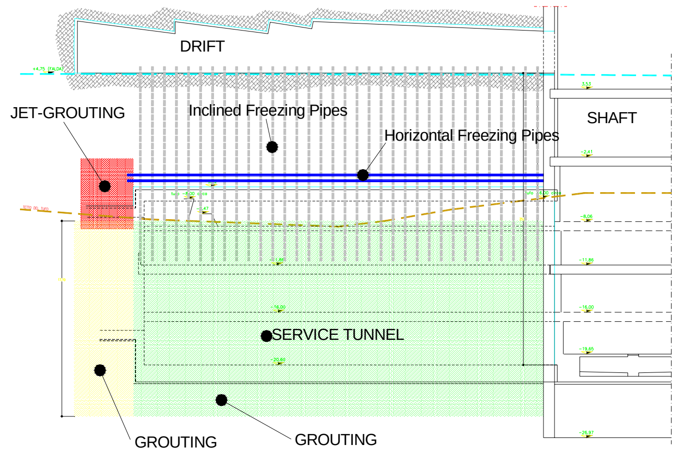


*Fig. 8. Longitudinal section of service tunnel - Distribution of the three different soil/rock improvement techniques.*

permeation grouting as a viable solution for the rock improvement. Therefore, the design considered the application of three different technologies: the AGF, the permeation grouting and the jet-grouting. AGF and jet grouting were applied where the tunnel section includes loose soil, while the permeation grouting was applied to improve the tuff characteristics. Grouting and jet grouting were carried out from the drift above the crown. The drift, located above the water table, was excavated in *pozzolana* sand, in presence of the following treatments ahead of the face (see Fig. 7):

- steel forepoles,
- cement grouting by PVC sleeved pipes,
- fibreglass nails within the core,

associated with steel ribs and gunite as temporary lining.

The soil/rock improvement for the *service tunnel* was applied to two different design sections: *standard* and *end-plug*. Figure 8 shows a longitudinal section of the tunnel, the two design sections and the distribution of the three different improvement techniques adopted.

<u>Service Tunnel Standard Design Section</u>

The *standard design section* is located between the shaft diaphragm wall and the *end-plug section*. The soil/rock improvement was installed around the envelope of the excavation. The core of the tunnel section was not treated (see Fig. 9).

The crown, where the maximum excavation induced stresses are concentrated, is located within the layer of *pozzolana* sand. This soil was improved by an AGF treatment, utilizing a combination of horizontal freeze lances (installed from the shaft) and inclined freeze lances (installed from the drift). The two rows of 40 m long horizontal boreholes were drilled by means of Magnetic Directional Drilling method. Conventional drilling could not be utilized because of the anticipated deviation of the boreholes (due to presence of the loose soil) and the design geometry (the 2 rows were spaced only 0.5 m). The AGF is a reliable method of soil improvement, both from

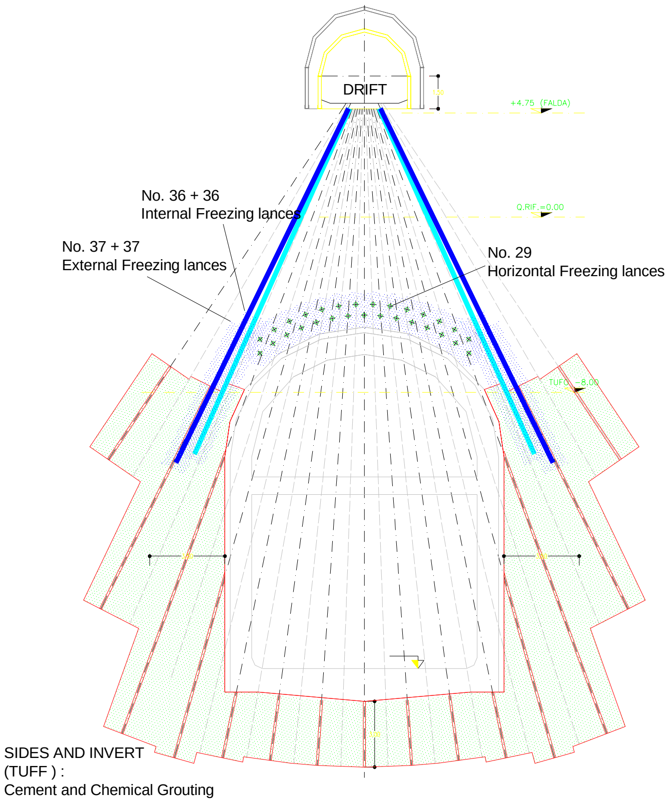


*Fig 9. Standard section of the Service Tunnel: Ground Freezing at the crown and permeation grouting at the sides and at the invert*

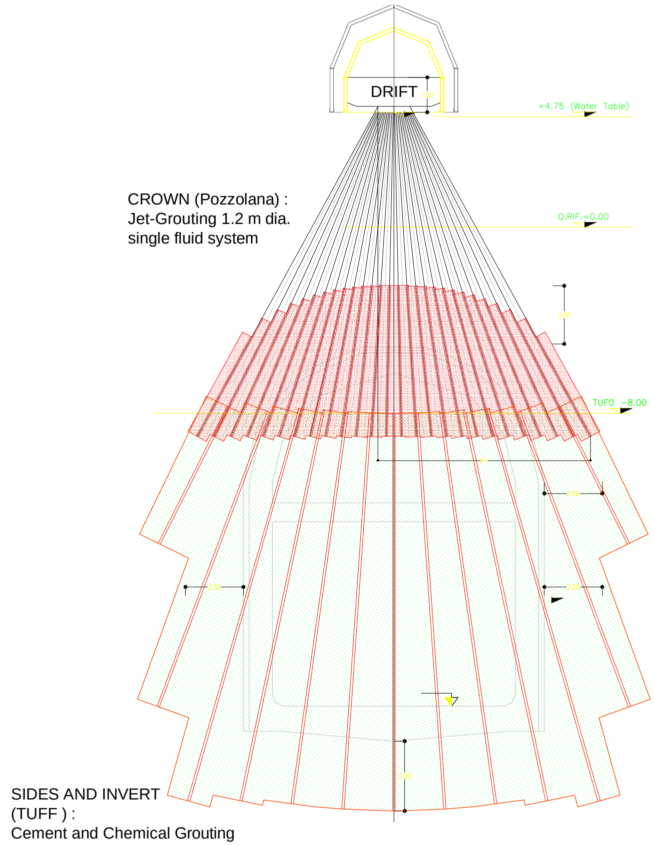


*Fig.10. End Plug section of the service tunnel: Jet-grouting at the crown and permeation grouting at the sides and at the invert*

the static and hydraulic point of view. With the AGF method, it was possible to build a supporting arch and reduce the permeability.

For the remaining part of the section, located within the tuff, the rock was improved by cement and chemical permeation grouting. The grouting treatment was carried out through inclined boreholes drilled from the drift. The boreholes pattern was 2.1 m x 1.1 m (measured at the bottom of the boreholes).

Service Tunnel End-Plug Design Section

The *end-plug section* is located at the end of the *standard section*. The end-plug section, having the function of bulkhead, was fully treated (see Fig. 10). Loose soil (*pozzolana*) was present at the crown, while tuff was present for the remaining part of the section. The loose soil at the crown was improved by jet grouting, to give both a structural and hydraulic function to the treated soil. The 1.2 m dia. jet grout columns were installed on a pattern of 0.64 m x 0.56 m (measured at the bottom of the columns). In order to minimize the impact of jet grouting, a single fluid method was utilized. The mix utilized was a pure cement suspension with C/W = 1. The remaining part of the section was treated by cement and chemical permeation grouting.

## GROUTING

Grouting is a technique utilized to modify the mechanic (strength and deformability) and hydraulic (permeability) characteristics of porous soils and fissured or fractured rocks (by permeation), or rocks having large cavities (by filling), or low permeability soils (by *claquage* technique).

From the rheological point of view the main classes of grouts, in order of increasing penetrability, are [Tornaghi et al., 1988]:

a) particulate suspensions (Binghamian fluids);
b) colloidal solutions (evolutive Newtonian fluids);
c) pure solutions (non-evolutive Newtonian fluids).

A suspension is usually called *stable* when bleeding is negligible, as required in general for the treatment of granular soil. Stabilized thixotropic grouts have both cohesion (yield strength) and plastic viscosity increasing with time at a rate that may be reduced by fluidifiers and retarders, but more consistently increased by filtration under injection pressure.

For the consolidation of the *service tunnel* the *MISTRÀ* cement mix and the *SILACSOL* chemical silica mix were used. Their properties are illustrated in the following paragraphs.

MISTRÀ Cement Mix

The main obstacles to the penetrability of a stable suspension are related to [Tornaghi et al, 1988]:

- the maximum actual particle size of the solid components in the injected grout, considering also the tendency of single grains to agglomerate thereby forming flocculent masses larger than the single dry particle [De Paoli et al., 1992];
- grout plastic viscosity and cohesion;
- the filtration rate which may involve a quick clogging even under low injection pressure.

The first obstacle was overcome by utilizing finer cements (Blaine specific surface over 5000 $cm^2/g$) and minimizing grain agglomeration by addition of a dispersing agent. However, the filtration problems remained unsolved, since in conventional stable grouts (type C in Fig. 11) the reduction of water loss rate can be obtained only at the cost of increasing viscosity by an additional content of colloids such as bentonite. Usual chemical additives (i.e., fluidifiers, retarders, dispersing agent) reduce viscosity but the filtration rate remains considerable (type C' in Fig. 11). Researches on various type of products (cement, bentonite and additives) led to the development of a class of grout named MISTRÀ (type B in Fig. 11) with the following main properties:

- no bleeding;
- filtration rates much lower than those of conventional stable mixes, even at very low viscosity;
- possibility of keeping the yield strength low over an adjustable period of time (up to many hours, if required);
- possibility of increasing the long term strength and reducing the permeability, as compared to conventional stable grouts with the same cement content.

As far as the composition is concerned, the C/W ratio may range between 0.3 and 1.2. The overall content of colloidal additive is generally within 0.5% and 5% of the weight of water. Therefore, the rheological and long term properties may widely vary according to specific requirements. In any case, the filtration rate remains lower than all the other types of grout, as emphasized in the left graph of Fig. 11). In Table 4 the characteristics of the MISTRÀ mixes adopted for the grouting at the *service tunnel* are shown.

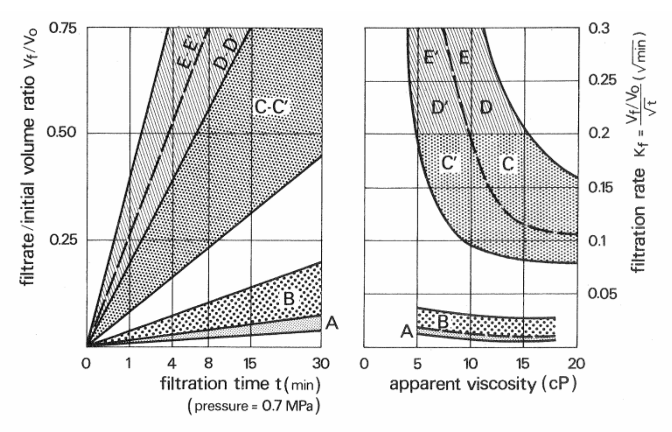


*Legend:*
*A : Bentonite muds;*
*B : Cement grouts with special colloidal additive (MISTRA');*
*C : standard Cement- Bentonite grouts;*
*D : poorly stabilized cement grouts;*
*E : unstable cement grouts;*
*C', D', E' : types C, D, E with fluidifiers and dispersing agent..*

*Fig.11. Ranges of significant rheological properties for various type of particulate suspensions*

*Table 4: MISTRA' Grout Characteristics at the Service Tunnel*

| | | |
|---|---|---|
| Composition | Cement/Water | 0.8 ÷ 1.2 |
| | Bentonite/Water | 0.5 ÷ 2.0% |
| Bleeding (%) | | 0 ÷ 2% |
| Marsh Viscosity(sec.) | | 35 ÷ 45 |
| Rheometer Parameters | Apparent Viscosity | 8 ÷ 12 |
| | Plastic Viscosity | 5 ÷ 8 |
| | Yield Strength | 1,5 ÷ 5 |
| Filter press test at 0,7 MPa | Filtrate (cm3) after 30' | 36 ÷ 72 |
| | Filtration Rate (mm1/2) | 0,016÷0,032 |

SILACSOL Chemical Mix

The best known colloidal solution consists of more or less diluted sodium silicate with inorganic or organic reagents, producing soft to hard silica gel. This is an "evolutive" mix, meaning that the viscosity of the mix increases before setting at a rate depending on dilution. Chemical solutions based on sodium silicate with inorganic reagents can produce only soft gels for waterproofing of sands, because of the high dilution.
The introduction of organic reagents allowed the adjustment of the setting time independently from silicate concentration. Soft to hard gels can be obtained according to the silicate/water ratio used. Further improvements were made in the quality of reagents, so to limit silicate concentration and better control syneresis (i.e., contraction of the gel and release of fluid) and creep phenomena. The syneresis phenomenon is negligible in medium fine sands. In gravel and coarse sand, the larger voids can be filled by a preliminary injection of particulate suspension. Therefore, a properly designed treatment would minimize gel dissolution and groundwater pollution. Nevertheless, the bad long-term performance in

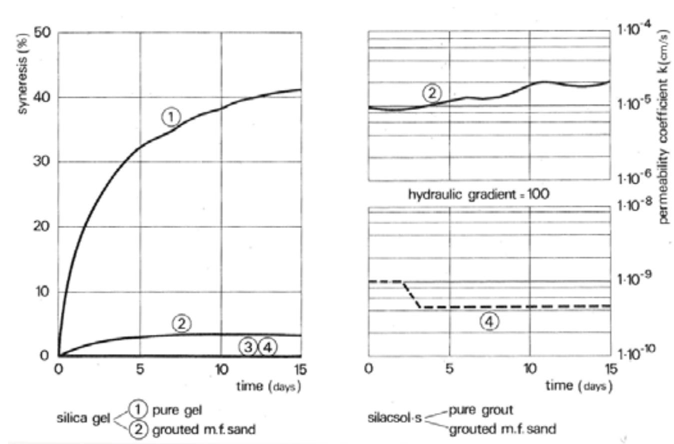


*Fig.12. Effect of the time on the syneresis and permeability of typical SILACSOL grout*

some cases of inadequate design or unskilled execution, and the consequently more and more strict specifications on organic chemicals, led to the research and development of a type of grout (SILACSOL) composed of an activated silica liquor and a calcium based inorganic reagent [Tornaghi et al., 1988].

Differently from commercial alkaline sodium silicates, which are aqueous solutions of colloidal silica particles, the liquor is a true silica solution. The activated dissolved silica, associated to the mineral reagent, produces calcium hydro-silicates with a crystalline structure quite similar to that obtained by the hydration and setting of cement. The result product is a complex of permanently stable crystals. Hence the reaction is not more an evolutive *gelation* involving the formation of macromolecular aggregates and possible loss of silicized water (syneresis). On the contrary, it is a direct reaction on molecular scale. This class of mixes have the same groutability range of common silica gels, allowing uniform treatment of medium to fine sands. Figure 12 is a typical viscosity/time curve that shows a Newtonian behaviour at fairly low viscosity, up to an effective groutability time of 50 min. Afterwards, the yield strength increases with time up to the final setting. Even in case of larger voids or fissures created by hydro-fracturing, a permanent filling is assured without any risk of syneresis. The activated silica mix has the stability of cement grouts, preventing ground water pollution. Other outstanding features of soil grouted with SILACSOL are the far lower permeability and the better creep behaviour, in comparison with the same soil grouted by means of a traditional silica gel. The permeability coefficient decreases from $10^{-5}$ cm/s with the silica gel to $10^{-10}$ cm/s with the SILACSOL. In addition, the permeability of the soil grouted with SILACSOL remains quite constant over extended periods of time under a hydraulic gradient as high as 100 (Fig. 12).

## Grouting Method

Different grouting methods may be applied according to the different circumstances encountered [Manassero, 1993].

In rock:

- Up-Stage or Down-Stage methods;
- Multi Packer Sleeved Pipe method (MPSP);

In soil:

- sleeved pipe method (i.e. *tubes à manchettes* method or TAM).

In rock, up-stage and down-stage methods are very efficient but also very expensive in terms of time and resources. On the other side, the technique normally adopted to grout the loose soil is not applicable to the rock because the stiffness of the rock prevents the breaking of the cement grouted sheath around the grout pipe (necessary to inject through the sleeve).

For this reason, the multi packer sleeved pipe method (MPSP) was developed. It is a hybrid system, invented to permit the utilization of sleeved pipes for grouting of rock. It improves grouting operations in those rock formations where:

- caving of the drilled holes and pronounced weathering prevent the sealing off of sections of holes to be grouted at the design depth;

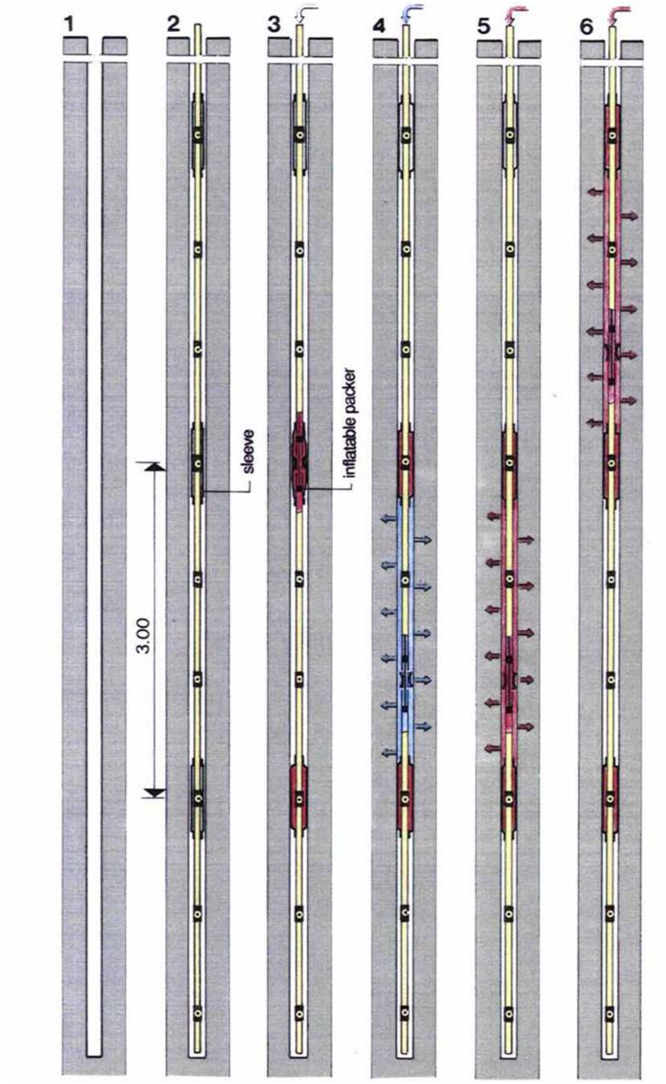


*Fig.13. MPSP grouting method*

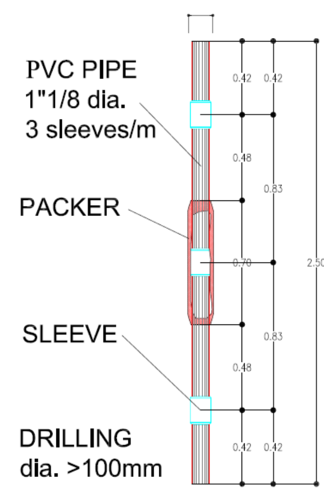


*Fig.14. Schematic of the MPSP utilized in this project.*

Fig 15. SILACSOL permeation through the cracks system as appeared during the tunnel excavation

- where the downstage method cannot achieve a sufficient consolidation and stabilization of the rock.

The MPSP method (Fig. 13) consists essentially in the installation of a plastic or steel pipe fitted at regular intervals with rubber grouting sleeves inside the borehole to be grouted. Bag packers, fastened to the grouting pipe at regular intervals (usually 2.5–5 m), seal off the sections to be grouted. The bag packers are expanded against the borehole walls by injection of grout into the bags. After the hardening of the grout in the packers, upstage grouting by means of double packer is performed. A schematic of the MPSP utilized for this project in shown in Fig. 14.

## GROUTING RESULTS

The maximum anticipated volume of the two grout mixes (cement and chemical) was 25% of the theoretical volume of soil to be treated. The C/W ratio of the cement mix was modified during the grouting process on the basis of the grout takes. The scope of the cement grouting was to fill the thicker cracks and fissures before the chemical grouting took place. The SILACSOL grout had to flow within a partially grouted material. Due to its very high penetrability, the SILACSOL grout was able to permeate the more thin cracks, not permeable to MISTRÀ grout (see Fig.15).

During the grouting, the following parameters were recorded automatically by a computerized system, in order to allow a reliable analysis of the results:
- progress of absorbed volume vs. time;
- trend of grouting pressure vs. time.

Two main characteristic parameters were associated to each sleeve: V (actual grout take per step) and P (actual average grouting pressure within the step); according to these parameters, the total number of injected sleeves was distinguished in four different categories:

*Table 5: Grout take results*

**First Grouting Phase**

| Area | Grout mix | Volume (l) | Volume (%) – part.– | Volume (%) – tot. |
|---|---|---|---|---|
| End-plug section | Mistrà | 13.223 | 0,73% | 20,33% |
| | Silacsol | 195.848 | 10,77% | |
| Standard section | Mistrà | 139.036 | 3,06% | |
| | Silacsol | 944.978 | 20,80% | |

**Second Grouting Phase**

| Area | Grout mix | Volume (l) | Volume (%) - part. | Volume (%) - tot. |
|---|---|---|---|---|
| End-plug section | Mistrà | 0 | 0,00% | 14,85% |
| | Silacsol | 169.421 | 9,32% | |
| Standard section | Mistrà | 0 | 0,00% | |
| | Silacsol | 775.202 | 17,06% | |

**Total Grout Volunes**

| Area | Grout mix | Volume (l) | Volume (%) - part. | Volume (%) - tot. |
|---|---|---|---|---|
| End-plug section | Mistrà | 13.223 | 0,73% | 35,17% |
| | Silacsol | 365.269 | 20,09% | |
| Standard section | Mistrà | 139.036 | 3,06% | |
| | Silacsol | 1.720.180 | 37,86% | |

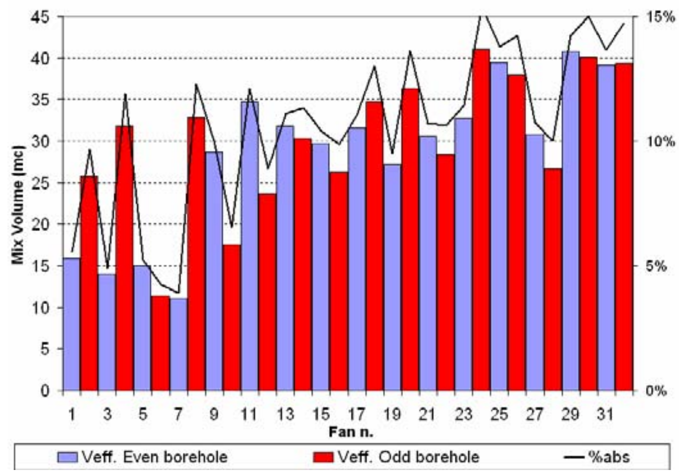


Fig.16. Second Grouting Phase: grout takes and percentage of theoretical volume of soil treated by grouting.

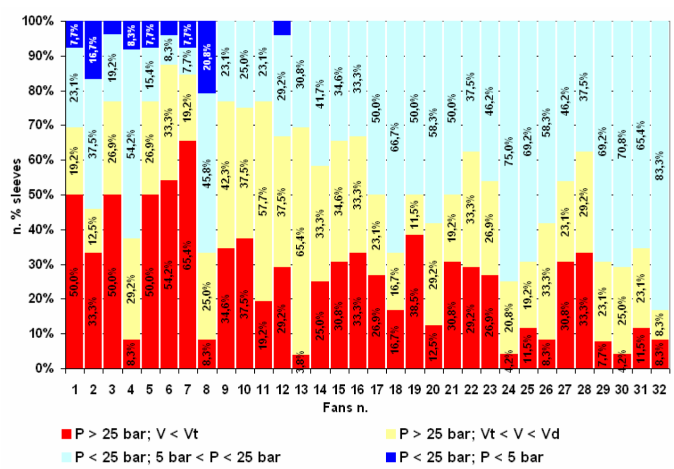


Fig.17. Second Grouting Phase: Percentage number of sleeves distributed by categories.

a) $P \geq P_{max}$ $V \leq V_t$;
b) $P \geq P_{max}$ $V_t < V < V_d$;
c) $P_{th} \leq P < P_{max}$ $V = V_d$;
d) $P < P_{th}$ $V = V_d$;
where :
$P_{max}$ = maximum grouting pressure, or refusal (25 bar);
$P_{th}$ = reference threshold grouting pressure (5 bar);
$V_t$ = theoretical volume of the borehole (30 l/stage);
$V_d$ = design volume.

The grouting works were carried out through 32 fans located in the standard section and 5 fans located in the end-plug section.

The numbering of fans started from the end-plug section and proceeded towards the shaft. In the end-plug section the odd fans (primary) were grouted with MISTRÀ, while the even fans (secondary) were grouted with SILACSOL. In the standard section the even fans (primary) were grouted with MISTRÀ and the odd (secondary) with SILACSOL. Primary and secondary fans were included in the first work phase. The analysis of the grouting data showed that the system of fractures included cracks too thin to be filled by cement mix, but groutable with chemical mix. A further Lugeon test provided the residual permeability of the treated tuff after the first phase of grouting. The results were not considered satisfactory, and convinced the Engineer to introduce a second grouting phase, in order to reduce the residual permeability of the rock mass. New semi-fans were then drilled between the fans of the first phase.

The SILACSOL mix was utilized in the second phase because it was considered the only grout able to provide efficient results. The Table 5 illustrates the general data of the grouting treatment in terms of volume and percentage of grout takes.

The diagram in Fig. 16 shows the grout (SILACSOL) takes and the percentages of the theoretical volume of soil treated by the second grouting phase. The diagram shows that the average percentage is 14.8%. This value is significantly higher than the expected value (6÷8 %).

Figure 17 shows the percentage of sleeves distributed by categories, as previously described. The diagram shows a significant residual number of sleeves belonging to category c) and d), even if this number is lower than what was achieved in the first grouting phase.

## ARTIFICIAL GROUND FREEZING TECHNIQUE

The Artificial Ground Freezing is a soil improvement method usually adopted to form a shell of frozen soil around an open excavation, protecting the excavation from collapses or intrusion of groundwater and loose soil. In principle, the technique foresees the installation within the soil of a system of freeze-lances properly spaced along the perimeter of the excavation area.

The primary scope of the AGF is to extract heat from the ground until its temperature is decreased below the freezing point of the groundwater system (freezing phase) [Harris, 1995]. Each freeze-lance forms a column of frozen soil. The column grows and merges together with the adjacent ones,

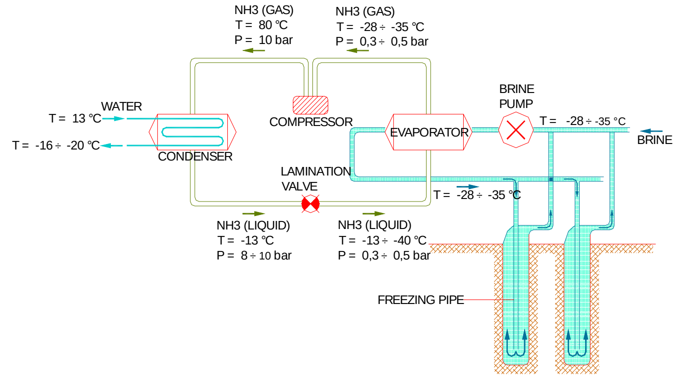


*Fig.18. Indirect system - Brine cooled by a refrigeration plant*

forming a resistant and low permeability retaining structure. Then, the achieved level of temperature is maintained by adjusting the flux of heat extracted from the soil (maintenance phase) until the excavation and construction activities are completed. Freezing is achieved by circulating a cooling fluid through the freeze-lances. The lances are made of two concentric pipes: the outer one has a closed end while the inner one is open. Generally, the cooling fluid is pumped through the internal pipe down to its deepest point. On its way back through the annulus between inner and outer pipes, the cooling fluid extracts the heat from the ground, thus decreasing its temperature.

Three different methods of artificial ground freezing are available.

The Brine method (see Fig. 18) is a closed process that requires the use of industrial refrigeration plants, connected to a coolant system, which consists of a brine pump, surface manifolds and freeze-lances installed into the ground. The outer and inner pipes forming the freeze-lance are typically made of steel and polyethylene, respectively. The brine, usually a calcium chloride ($CaCl_2$) solution, is cooled by the refrigeration plant, typically at temperatures of -25 to -40°C, and pumped into the closed circuit. The warmer brine returning from the freeze-lances through the insulated surface manifold system is then re-cooled and re-circulated into the closed circuit [Crippa and Manassero, 2006].

The Liquid Nitrogen (LN) method (see Fig. 19) is an open process. The cooling medium is LN at -196°C. Both the outer and inner pipes are made of either copper or stainless steel. The LN is pumped directly into the freeze-lances through the

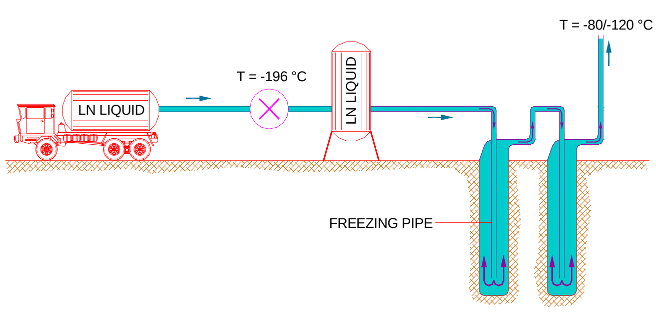


*Fig. 19. Direct system – Liquid Nitrogen method*

manifold system. On its way along the freeze-lances the LN evaporates and then the resultant gas is allowed to exhaust into the atmosphere, at a temperature ranging from -100°C and -60°C. A third method consists of a combination of the two methods described above: the LN method is applied during the freezing phase and the brine method during the maintenance phase.
The choice of the freezing method to be adopted is a function of a number of design, construction and economical factors, as the required static strength of the frozen ground, the available time for freezing, the duration of the freezing maintenance period, logistics, costs, etc. [Gallavresi, 1991].

## GROUND FREEZING AT TOLEDO STATION

At the Toledo *service tunnel* the combination of the two methods was used: LN for the freezing phase and brine for the maintenance phase.
The freeze-lances utilized were composed by a 76 mm dia., 2 mm thick external copper pipe. During the freezing phase, the internal pipe was made of a 18 mm dia., 1 mm thick copper pipe. During the maintenance phase, the internal pipe was replaced with a 50 mm dia., 4 mm thick polyethylene pipe.
The LN was fed to the freeze-lances at -196 °C, while the brine was circulated at a temperature within the range -28 ÷ -35 °C.
he scope of AGF at the Toledo *service tunnel* was to protect the first excavation phase of the tunnel crown. The excavation of the sides and the invert was achieved in two successive phases. The following layout of the freezing-lances was utilized (see 3-D schematic in Fig. 20):

- 16 + 15 horizontal lances, 40 m long, drilled by Horizontal Directional Drilling method (HDD) ahead of the face from the access shaft, located around the crown;
- 73 + 73 sub-vertical lances, 18 m long, drilled from the drift, located along four lines parallel to the tunnel and with the toe embedded into the treated tuff; only the lower 7 m were active, while the upper stretch was insulated.

Pictures of the equipment during the drilling of the horizontal freeze-lances and the manifold system at the tunnel face in the shaft and inside the drift are shown in Fig. 22, 23 and 24.

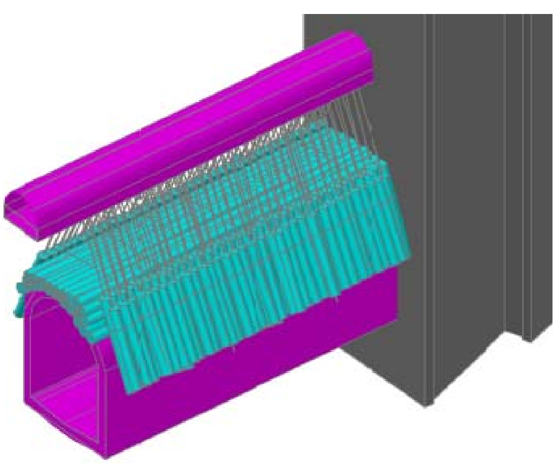

*Fig. 20- 3-D schematic of the frozen shell*

*Fig. 21. Equipment during the drilling by HDD for horizontal freeze-lances installation.*

*Fig. 22. Manifold system at the tunnel face and horizontal freeze-lances*

*Fig. 23. Drift manifold system and inclined freeze-lances*

Two different distribution plants and manifolds were installed. They were composed of feeding and return pipes and manifold.
The Liquid Nitrogen was stocked in thermal silos placed at the surface level. In the indirect system, that is a closed circuit system, only brine at liquid state flows. Two refrigeration plants, one linked to the lances located into the drift and the other one linked to the pipes located on the front of the tunnel, were installed on a middle floor of the shaft.
Two ammonia refrigeration plants were utilized during both the freezing and maintenance phase. Each refrigeration plant included the following main elements:

- screw compressor, which operates at a temperature between -28 and -35 °C for evaporation and +37°C for condensation, driven by a 220 KW electric motor;
- heat exchanger oil cooler that works with the water of the evaporator tower;
- heat exchanger that works with the brine;
- ammonia separator;
- evaporator condenser (evaporator tower with cooling water circuit);
- two electric pumps for brine circulation.

The electric power hook-up for each refrigeration plant is about 300 KW. A generating plant of 450 kVA capacity is required to drive the refrigeration plant. The evaporator tower requires a supply of approximately 750 litres of water per hour. The water should not contain sediments to avoid the plugging of the circuit of the evaporator. Each plant has a freezing capacity of about 234 kW with brine chilled at the nominal temperature of -35°C. A safety system, which continuously monitors the proper functioning of the plant, is in operation.
The feeding Liquid Nitrogen circuit includes 42.16 mm dia., 2.77 mm thick stainless steel pipes. The return plant utilizes 6 in dia. steel pipes, to facilitate the evacuation of the exhausted gas. As far as the feed and the return brine plant are concerned, polyethylene insulated tubes with an internal diameter of 180 mm were used, in order to reduce the dispersion along the circuit.

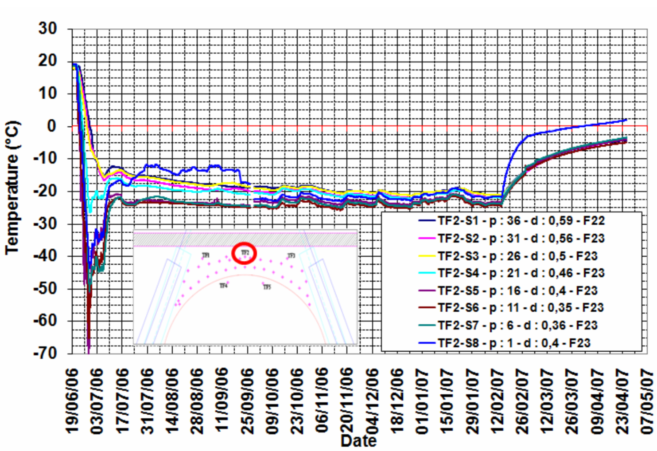


*Fig.24. Typical Temperature - Time graph (chain TF2)*

TEMPERATURE MONITORING AND PROCESSING.

The data acquisition system utilized for the AGF control was mainly composed by thermometric chains, data loggers and software for data acquisition, recording and processing. In order to monitor the temperature state of the soil and the growing of the columns of frozen soil around the pipes, thermometric chains (TMC), containing a certain number of thermometric sensors, were installed within suitable pipes sub-parallel to the freeze-lances. When possible, the TMC were placed at a variable distance from the nearest freeze-lance. The sensors were thermo-resistances of the PT1000 type with accuracy of 0.01°C. Five TMC, with 8 sensors at 5m spacing, were employed to monitor the growth of the freezing activated from the shaft. Eight TMC, with 6 sensors at 2 m spacing, were utilized to monitor the freezing activated from the drift. The temperature measurements were taken every 30 minutes. The dedicated software was able to produce diagrams of the ground temperature as a function of time, position, distance, etc.
Two types of representation were drawn:

- Temperature vs. time diagram;
- Temperature vs. depth diagram.

The temperature versus time diagram represents the trend of the soil thermal conditions during the whole freezing activity.
In Fig. 24, a typical Temperature-Time diagram, the three phases of the ground freezing process can be observed:

- The freezing phase, activated by using the LN system. The temperature of the soil goes down to very low values due to the very high cooling power of LN that operates at a temperature of -196 °C. The scope of this phase is to reach the thermal conditions of the soil required by the design. The excavation operation started just after the end of this phase.
- The maintenance phase, by brine method. The temperature remains stable at almost the same level. An equilibrium between the heat extracted from the soil and the heat lost by the frozen body is established.
- The thawing phase, without any freezing system working. The temperature increases up to the natural temperature of the soil at the end of the phase (the temperature monitoring was interrupted before the completion of this phase).

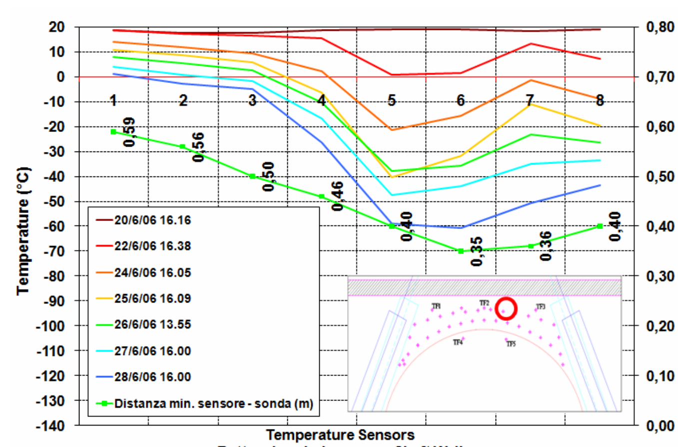


*Fig. 25. Typical Temperature - Depth graph (chain TF2)*

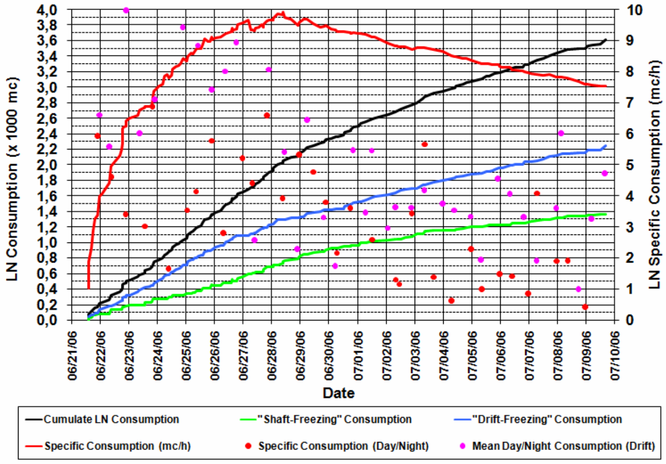


*Fig. 26. Liquid Nitrogen Consumption*

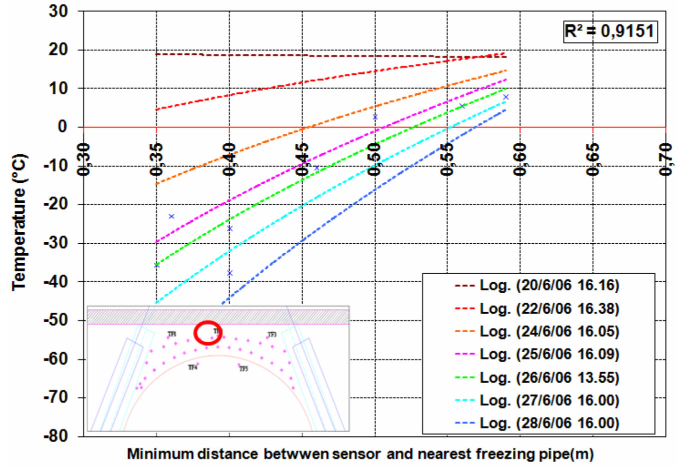


*Fig. 27. Typical temperature vs. minimum distance between sensor and nearest freeze-lance (chain TF2)*

In Fig. 25, where a typical Temperature-Depth diagram is illustrated, the curves show the trend of temperature along the TMC. In the same graph, the green curve represents the distance of each single sensor from the nearest freeze-lance. Comparing these curves we should find a similar shape, if there are no factors affecting the freezing process (in particular, if there is no significant water seepage through the soil to be frozen). Differences between the curve shapes indicate that there are factors disturbing the heat transmission.
The consumption of Liquid Nitrogen during the freezing phase is shown in Fig. 26. The graph shows a total consumption of 3.6 million liters of LN, of which 38% was consumed for the shaft-freezing and 62% for the drift-freezing. The average consumption per hour ranged from 10000 l/h when all the cryogenic valves of the freeze-lances were totally opened, to 2.000 l/h when they were partially closed. The main characteristic parameters of the freezing phase are described in Table 6.
Interpretations on the growing of the frozen soil columns can be made considering a hypothetical behaviour modelled by the heat transmission law in an isotropic and homogeneous soil.
A first kind of interpretation may be provided by drawing a logarithmic interpolation of measured temperatures vs. distance from the nearest freeze-lance for each thermometric chain. This curve may represent the temperature gradient around the hypothetical freeze-lance, identified by the Y axis. The intersection with the X axis gives the distance from the lance to the 0°C isotherm that physically represents the radius of the frozen soil column (see Fig. 27). The sequence of these points gives the growing of the columns dimension vs. time. The determination of this curve is based on the temperature measures without considering any boundary condition.

*Table 6: Main characteristic parameters of the freezing phase*

| Zone | LN total volume $V_{LN}$ (m³) | Total freeze-lances length $L_p$ (m) | Nominal frozen soil volume $V_{FS}$ (m³) | Time T (days) | $V_{LN} / V_{FS}$ (l/m³) | $V_{LN} / L_P$ x T (l/mxh) |
|---|---|---|---|---|---|---|
| SHAFT | 1364 | 1240 | | | | |
| DRIFT | 2251 | 2628 | 4300 | 19 | 840,7 | 2,0 |
| TOTAL | 3615 | 3868 | | | | |

An other interpretation considers that the temperature gradient around the freeze-lances in steady condition is described by a curve calculated with a logarithmic interpolation between the temperature measure of each singular sensor and the boundary conditions represented by the temperatures of the freeze fluid and of the natural soil. This curve is composed by two different branches, also modelled by a logarithmic curve, which equation is [Sanger and Sayles, 1979]:

$$T = a + b \ln x \qquad (1)$$

where the constants $a$ and $b$ are calculated imposing appropriate boundary conditions.
With reference to Figure 28, the first curve (N. 1) is drawn within the frozen soil (T < 0°C), where the distance from the freeze-lances *r* is lower than the radius of the frozen soil *R* (T = 0°C); the second curve (N. 2) is drawn within the unfrozen

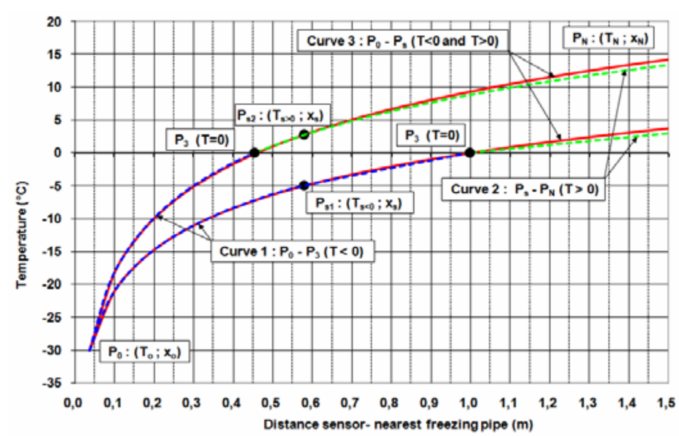


*Fig. 28 Typical temperature gradient around a freeze lance according to Sanger and Sayles, 1979.*

soil (T > 0°C), where the distance is higher than R. The intersection between the two branches (P3) is coincident with the intersection on the X axis (T = 0°C). A unique curve (N. 3), which equation is of the same type, is drawn close to the two above described branches, with a negligible error. It considers the following boundary condition:

$$\begin{cases} x_1 = x_s \\ T_1 = T_s \end{cases} \qquad \begin{cases} x_2 = x_0 \\ T_2 = T_0 \end{cases} \tag{2}$$

where:
$x_s$: distance of the thermometric sensor from the nearest freeze-lance; $T_s$: temperature measured by the sensor; $x_0$: radius of the freeze-lance; $T_0$: temperature at the freeze-lance external surface.
The scope of this elaboration is to determine the distance x where the temperature is -2°C, that is a conventional value assumed conservatively as boundary of the frozen body.
By means of this kind of interpretation it is possible to create hypothetical surface of:

- temperature of all the points whose distance from the nearest freeze-pipe is a determined r (isotherm curves at a prefixed isometric); an example is shown in Fig. 29, where the pre-determined distance is 0.7 m;
- distance of all the points whose temperature is a pre-determined value (isometric curves at a prefixed isotherm; e.g. T = -2°C).

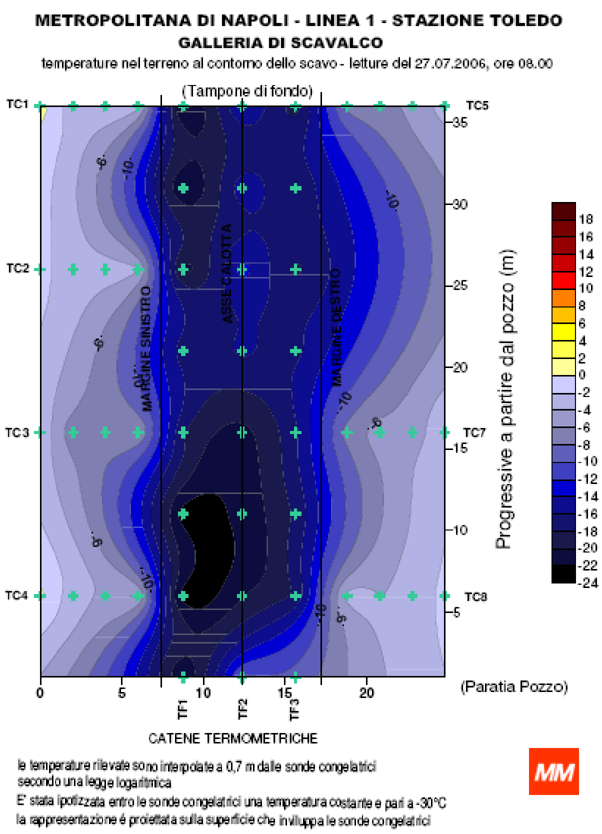


*Fig. 29. Typical representation of isotherm curves at a prefixed isometric.*

## CONCLUSIONS

The excavation of the Toledo *service tunnel* was carried out in three different phases: crown, sides and invert. The freezing shell, obtained during a 19 days freezing phase, was maintained for the whole duration of the first two phases (7 months).
The whole excavation, protected by rock grouting and artificial ground freezing, was carried out in substantially dry conditions. The soil improvement methods adopted proved to be extremely effective and particularly suitable for the soil/rock materials present on site.
The impact of the soil improvement and excavation works on the adjacent buildings and utilities was negligible. The lowering of the water-table in the neighbourhood due to the specific activity of tunnel excavation resulted negligible.

## REFERENCES

Cavagna, B., G. Colombo and A. Sciotti [2004]. "*The use of EPB TBM for tunnel digging in soft rock: the example of Naples underground*". *Proceeding of International Congress on Mechanized Tunnelling: challenging case histories*. Turin.

Crippa, C. and V. Manassero [2006]. "*Artificial round freezing at Sophiaspoortunnl (The Netherlands). Freezing parameters: data acquisition and processing*". *ASCE Geocongress 2006 Geotechnical Engineering in the Information Technology Age*. Atlanta, GA. February 26-March 1

De Paoli, B., B. Bosco, R. Granata and D.A. Bruce, [1992]. "*Fundamental observations on cement based grouts: traditional materials*". *Proc. Conference on Grouting. Soil Improvement and Geosynthetics.*, New Orleans. February 25-28. Geothec. Spec. Pubbl. No. 30 ASCE, pp 474-485.

Gallavresi, F. [1991]. "*Considerations on the choice among the different freezing methods and competitiveness of the system as compared to alternative solutions*". *Proc. 6th International Symposium on Ground Freezing*. Beijing, September 10-12. Balkema.

Harris, J.S. [1995]. "*Ground freezing in practice*". Thomas Telford

Manassero, V. [1993]. "*Different techniques for soil improvement and underpinning*". *International Symposium on Novel Foundation Techniques*. EC Science Programme Symposium, Cambridge, UK. September 2-3.

Sanger, F.J. and, F.H. Sayles [1979]. *"Thermal and rheological computations for artificially frozen ground construction"*. Engineering Geology, 13, 311-337.

Tornaghi, R., B Bosco and B. De Paoli [1988]. *"Application of recently developed grouting procedures for tunnelling in the Milan urban area"*. *Fifth International Symposium on Tunnelling* – April 18-21. London.